



Lithium Orthosilicate-Linear Low-Density Polyethylene Nano-Composite as Substrate for High Frequency Devices: Dielectric Characterization

Pulin Dutta & Kunal Borah*

Department of Physics, North Eastern Regional Institute of Science and Technology (Deemed to- be-University), Nirjuli, Itanagar, Arunachal Pradesh 791 109, India

Received 23 April 2022; accepted 13 September 2022

Dielectric properties of nanosized Lithium Orthosilicate (Li_4SiO_4) and linear low-density polyethylene composite at X-Band frequencies are investigated, to realize its utility as a substrate for microwave devices. Solid state technique is used to synthesize nano Li_4SiO_4 . To confirm the structural and morphological properties of the synthesized nano Li_4SiO_4 , X-ray diffraction, Fourier transformed infrared spectroscopy and transmission electron microscopy are used. Composites of nano Li_4SiO_4 and linear low-density polyethylene matrix are synthesized with varying weight fraction of nano Li_4SiO_4 viz. 2%, 4% and 6%. The lateral portion of a fractured sample (composite) is examined using scanning electron microscope to confirm homogeneous dispersion of nano Li_4SiO_4 in linear low-density polyethylene matrix. Water absorption measurement of all the composites are carried out based on ASTM D570-98. Densities of the composites are measured via hydrostatic weighing by using Archimedes principle. Complex permittivity and permeability measurement of the composites are recorded by utilizing Nicholson-Ross approach. For all weight fraction of the nano inclusions, the real component of permittivity and dielectric loss tangent of the composites in the X-band are found to be in the range of 2.2 – 2.6 and 10^{-2} – 10^{-4} , respectively. Return losses for the composites are calculated from complex permittivity and permeability values to validate its applicability as substrate for various high frequency applications.

Keywords: Complex permittivity; Complex permeability; Return loss; X-band

1 Introduction

With the growth of electronic industries, the demand of tailored substrates for high frequency devices has increased manifold.¹ The complex permittivity and permeability of any material determines its suitability as substrates for these devices. A single material substrate may not always be able to satisfy all the requirements for a certain application. Various composites, such as inclusion filled polymer matrix (nano, ceramic, dielectric magnetic, *etc.*) can be a viable choice.² Ceramics have high dielectric strength, moderate dielectric constant and low loss tangent.³ Hence, dielectric ceramic nano materials and polymer composites can be regarded as feasible microwave substrate materials for high frequency application.

Many ceramic nanomaterials, including Mg_2SiO_4 , $\text{Ba}(\text{Mg}_{1/3}\text{Ta}_{2/3})\text{O}_3$, $\text{Mg}_4\text{Nb}_2\text{O}_9$, ZnAl_2O_4 , *etc.*, have been studied for their interesting dielectric properties in microwave frequencies. Cerium oxide (CeO_2) filled polytetrafluoroethylene (PTFE) is synthesized for microwave substrate applications, using powder

processing technique by increasing CeO_2 volume fraction (%VF) up to 0.6%.⁴ Cavity perturbation technique is used to measure the microwave dielectric characteristics. For 0.6 %VF of filler loading the measured value of the real part of complex permittivity (ϵ') is 5 and dielectric loss tangent ($\tan\delta_e$) is 6.4×10^{-3} respectively at 7GHz. Dielectric properties of PTFE loaded with varying %VF of MgTiO_3 is studied.⁵ The measured value of ϵ' is 5.5 and $\tan\delta_e = 2.7 \times 10^{-4}$ (at 10 GHz) makes the composite, a promising material for electronic packaging. Dielectric properties with varying weight fraction (%WF) of titania (TiO_2) filled low density polyethylene (LDPE) composite is studied as a microstrip patch antenna (MPA) substrate in the X-band. The composite with 6% WF shows an increase in ϵ' from 2.13 to 2.5 with increasing frequency. The reported value of $\tan\delta_e$ is 4×10^{-3} making it a suitable substrate material for MPA. The discussed composite is used as a graded substrate, which as a result enhances the bandwidth and S11 of the antenna.⁶ A comparative investigation of dielectric behaviour of barium titanate (BaTiO_3) in X-band with polyaniline (PANI) and maleic resin as polymer

*Corresponding authors: (Email: kbnerist@gmail.com)

matrix is reported. It is found that a very small amount of BaTiO₃ in insulating PANI reduces the value of ϵ' and $\tan\delta_e$ up to 26 and 0.2. While in case of BaTiO₃-maleic resin the value of ϵ' and $\tan\delta_e$ decreases gradually with decreasing filler concentration and reached a minimum value of 2.3 and 0.3 respectively.⁷ X-band dielectric property of PTFE-TiO₂ is studied by cavity perturbation method by using nano sized and micron sized TiO₂. In the studies it is observed that ϵ' of nano sized composite is higher than the micron sized composite. It is also observed that ϵ' and $\tan\delta_e$ increases with %WF and reaches maximum value of 7 and 10^{-2} for 50%WF.⁸ A comparative dielectric study is done for PTFE matrix loaded with alumina (Al₂O₃) and magnesium oxide (MgO) in the X band for microwave substrate application. From the investigation it is found that PTFE-Al₂O₃ composite has a ϵ' of 4.30 and $\tan\delta_e$ of 2.1×10^{-3} whereas ϵ' and $\tan\delta_e$ of the PTFE-MgO composite is 3.35 and 1.5×10^{-3} respectively for optimum filler loading.⁹ Composite of barium strontium titanate (BST) and thermoplastic cyclic olefin copolymer is investigated with different loadings of BST, using bulk and nano sized ceramic powders for high frequency application. The value of ϵ' and $\tan\delta_e$ is measured as a function of filler loading at 1GHz. The result shows moderate value of $\epsilon' = 6$ and low value of $\tan\delta_e = 9 \times 10^{-3}$.¹⁰ Dielectric properties of CaTiO₃ loaded polypropylene composite fabricated through compression molding method are studied by using x-band cavity perturbation technique for microwave substrate application. The composite have an effective value of ϵ' and $\tan\delta_e$ is 11.74 and 7×10^{-3} respectively for highest filler concentration.¹¹ Dielectric properties of polystyrene -magnesium based ceramics (MgTa₂O₆, MgNb₂O₆, and MgWO₄) is investigated in the frequency range 1–7.3 GHz frequency for microwave substrate and electronic packaging application. The value of ϵ' is nearly constant reporting 25.48, 20.84 and 12.44 respectively for MgTa₂O₆, MgNb₂O₆, and MgWO₄ with $\tan\delta_e$ nearly 10^{-3} for all the materials.¹² A coplanar waveguide monopole antenna is fabricated over Ca[(Li_{1/3}Nb_{2/3})_{0.8}Ti_{0.2}]_{0.3-8} (CLNT)-epoxy composite. From the dielectric investigation it is observed that value of ϵ' increases with increase in CLNT concentration. The reported value of ϵ' and $\tan\delta_e$ for 0.4 %VF is 7.7 and 4×10^{-3} respectively at 9 GHz.¹³ High-density polyethylene (HDPE) and BaO-Nd₂O₃-TiO₂ (BNT) coated with LDPE

composite is synthesized and are used for microwave substrate applications. The composites ϵ' value decreased from 11.87 (at 7 GHz) to 3.45 (at 9 GHz), while $\tan\delta_e$ remain below 1.6×10^{-3} .¹⁴ Dielectric resonator structures for wearable devices on cyclic olefin copolymer (COC) and barium strontium titanate (BST) composites are studied at 2.45 GHz frequency. The ϵ' and $\tan\delta_e$ of BST- COC's are 14.5 and 2.35×10^{-3} , respectively.¹⁵ A multi-layer alumina-ceramic and polyimide substrate active resonating structure is proposed for wireless communication systems. At 10 GHz, the device is fabricated on a four-layer alumina-ceramic substrate having $\epsilon' = 9.0$ and $\tan\delta_e = 10^{-3}$, as well as a four-layer polyimide substrate with $\epsilon' = 3.2$ and $\tan\delta_e = 2 \times 10^{-2}$.¹⁶ It is seen that, substrates with ceramic included in a polymer matrix with varying %WF can be utilized for various high frequency devices. This report has exercised this fact, and investigated to fill the research gap related to selection of suitable ceramic material as fillers.

LLDPE is a polymer with linear qualities and acceptable electrical properties, as well as good tensile properties, chemical resistance, low water absorption, and high thermal stability. The decomposition temperature of LLDPE is 438.85 °C with weight loss of 0.01%. The major weight loss occurs in between the temperatures 441.98 and 513.15 °C due to growth of volatiles¹⁷⁻¹⁹. Silicates are recognized for their excellent dielectric characteristics, low loss tangent and minimal thermal expansion.²⁰ Chemical, physical, mechanical and magnetic properties of nano ceramics differ from other materials like metals and conventional bulk ceramic materials, this makes it a possible candidate for this investigation.

In this work, nano Li₄SiO₄ is synthesized and are used as inclusions in a linear low-density polyethylene (LLDPE) polymer matrix with varying %WF (viz. 2%, 4%, and 6%) to investigate its high frequency dielectric properties. Along with other structural and morphological studies, X band complex permittivity and permeability of composites (LLDPE-nano Li₄SiO₄) is measured using Nicolson Ross technique.

2 EXPERIMENTAL WORKS

2.1 Synthesis of nanosized Li₄SiO₄ and its composite with LLDPE

Nanosized lithium orthosilicates are synthesized by following conventional solid-state method by mixing

high purity ingredients of nanosized silica dioxide (SiO_2) and lithium carbonate (Li_2CO_3) (Sigma Aldrich) in stoichiometric proportions. Nano Li_2CO_3 and SiO_2 are mixed in 2:1 molar ratio in an agate mortar for 1 hour. The mixture is then calcined at 900°C for 4 hour.²¹ To make the composite, LLDPE is dissolved in toluene and stirred with a mechanical stirrer at 100°C . After dissolving the synthesized Li_4SiO_4 nano particles are added in WF increments of 2%, 4% and 6% to make a homogeneous mixture of the inclusions in the polymer. When the toluene is completely evaporated, a viscous solution is formed. The solution is then poured into a die with dimensions of $10 \times 22 \times 2 \text{ mm}^3$, allowed to congeal for 2 hours at room temperature, and a composite substrate of LLDPE-nano Li_4SiO_4 is obtained.²²

2.2 Structural and Morphological Characterization

The X-ray diffraction (XRD) patterns of nano Li_4SiO_4 is recorded using a Bruker D8 (Make: BRUKER AXS, GERMANY, Model: D8 FOCUS) X-ray powder diffractometer with $\text{Cu K}\alpha$ radiation ($\lambda = 1.5406$). Fig. 1 shows the XRD patterns of Lithium Orthosilicate nano particles. The peaks at $2\theta = 16.79^\circ$, 22.18° , 24.17° , 29.27° , 34.07° , 36.86° , 39.56° , 48.75° , 63.33° and 73.92° corresponding to the (h k l) value (1 0 0), ($\bar{1}$ 1 0), (1 0 1), (0 2 0), (0 2 1), ($\bar{2}$ 1 0), ($\bar{1}$ 0 2), ($\bar{2}$ 2 1), (0 4 1) ($\bar{2}$ 4 1), are the diffraction peaks of Lithium Orthosilicate (ICDD 00-037-1472). The sample has monoclinic structure, with lattice parameters of $a = 5.39$, $b = 9.39$, and $c = 4.66$. Along with the dominant Li_4SiO_4 peaks, some peaks of Li_2CO_3 are also observed due to incomplete reaction. The average crystallite size is calculated using Debye-Scherrer formula²³ and is found to be 150 nm.

FTIR spectra in the range of $400\text{--}4000 \text{ cm}^{-1}$ are obtained using a NICOLET FTIR spectrometer.

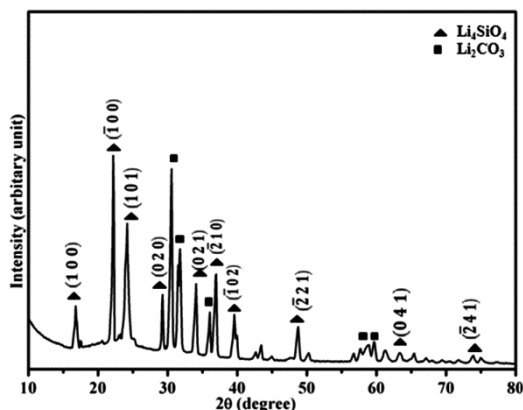


Fig. 1 — XRD of nano Li_4SiO_4 .

(Model: IMPACT 410) (Make: NICOLET). For this the material is mixed with KBr and crushed to a very fine powder and in a moisture-free environment, a transparent disc is created to obtain FTIR spectra. The FTIR spectrum of the synthesized Li_4SiO_4 is shown in Fig. 2. The -OH stretching vibration caused by physical adsorption of water and bound water is responsible for the broad characteristic band ranging from $3770\text{--}2480 \text{ cm}^{-1}$. The distinctive bands observed from FTIR measurements at $1186\text{--}1047 \text{ cm}^{-1}$ and 480 cm^{-1} correspond to Si-O-Si bending vibrations and O-Li-O stretching vibrations, respectively. The band observed around 862 cm^{-1} and 1423 cm^{-1} is due to the presence of carbonates in the form of Li_2CO_3 .

Transmission electron microscope (TEM) (Model: TECNAI G2 20 S-TWIN)(FEI COMPANY, USA) is used to confirm the average particle size of the synthesized Li_4SiO_4 . According to the TEM image in Fig. 3, the average particle size of nano Li_4SiO_4

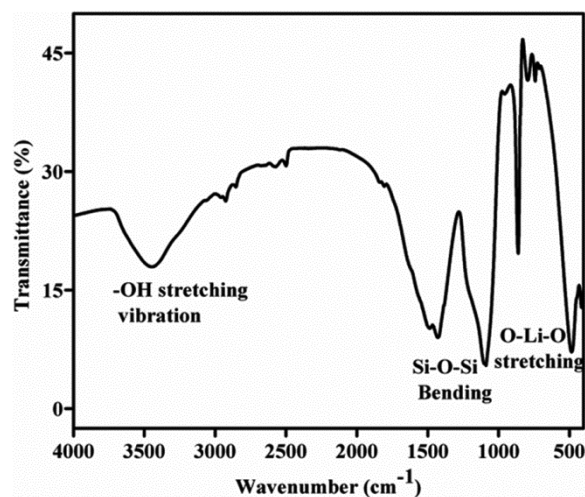


Fig. 2 — FTIR of nano Li_4SiO_4 .

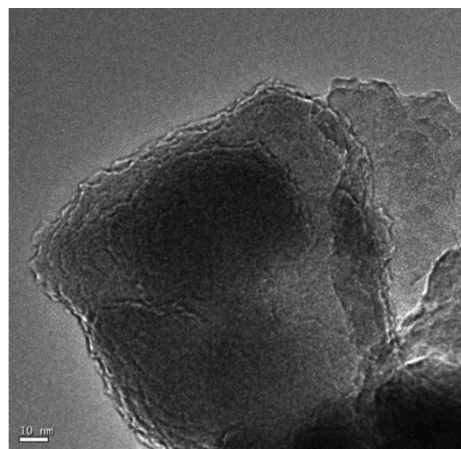


Fig. 3 — TEM of nano Li_4SiO_4 .

complements the calculated value obtained from Debye Scherrer formula. The lateral side of cracked samples of 6% WF is examined using a scanning electron microscope (SEM)(Model: JSM- 35CF, Make: JEOL) to validate the uniform dispersion of Li_4SiO_4 in LLDPE composite substrates (Model: JSM- 35CF, Make: JEOL). Fig. 4 shows SEM images of LLDPE-nano Li_4SiO_4 composite substrates. In some portions the agglomeration of nanomaterials has occurred during mixing due to high viscosity of LLDPE.

Adverse environmental circumstances, such as excessive moisture and temperature, can cause material characteristics to alter. So properties such as water absorbance, density, and coefficient of thermal expansion (CTE) must be investigated. Water absorption is measured according to ASTM D570-98, and the changing trend of percentage water absorption with time of immersion is shown in Fig. 5.²⁴

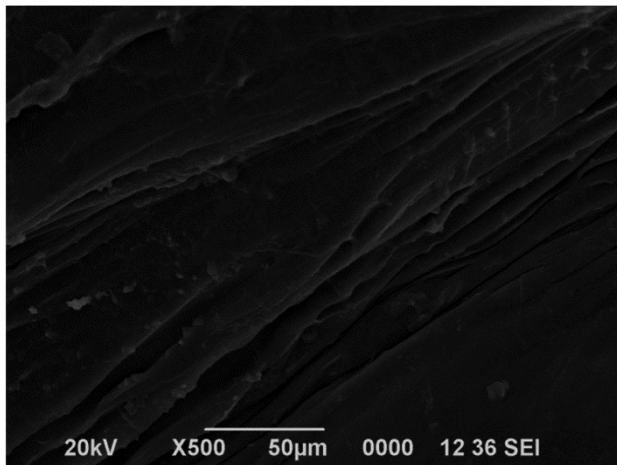


Fig. 4 — SEM of LLDPE- nano Li_4SiO_4 (6%) composite.

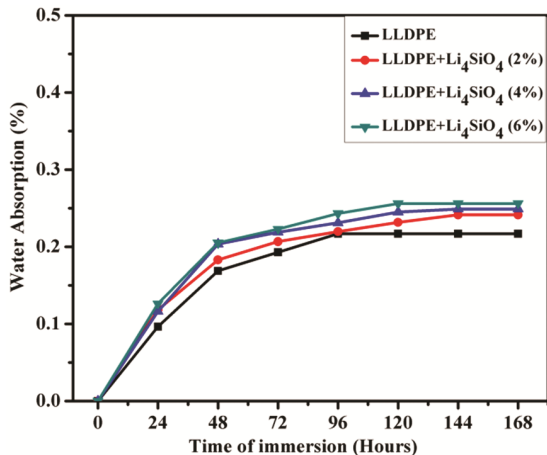


Fig. 5 — Water absorption of pure LLDPE and LLDPE- nano Li_4SiO_4 composite.

To measure the water absorption sample of size $10 \times 22 \times 2 \text{ mm}^3$ is immersed in water and weight is measured in a weighing balance of precision 0.0001 g after every 24 hr of immersion until saturation is achieved. The saturation is achieved after 168 hr of immersion. From the recorded weight the percentage of water absorption after each 24 hr of immersion is calculated by using equation (1) and the calculated values are given in Table 1. From the table it is seen that for the 6 %WF the saturation water absorption is only 0.25%.

$$w_a(\text{in } \%) = \frac{w_f - w_i}{w_i} \times 100 \quad \dots (1)$$

Where

w_a =Percentage of absorbing water.

w_f = Final weight of the pieces.

w_i = Initial weight of the pieces.

The densities of the composites are estimated by using Archimedes principle utilizing hydrostatic weighing.²⁵ For this, a half filled beaker with ethanol is weighted and the combined mass of beaker and ethanol is recorded (w_1). After that composite sample is suspended in ethanol and a fresh reading is taken (w_2). Finally, the sample is allowed to settle at the bottom of the beaker and reading of the combined mass is measured (w_3). The density is calculated using equation (2) by using the recorded values of w_1 w_2 w_3 and d (ethanol density).

$$\rho = \frac{w_3 - w_1}{w_2 - w_1} \times d \text{ (g/cm}^3\text{)} \quad \dots (2)$$

The obtained value of density is listed in Table 2.

The coefficient of thermal expansion (CTE) is an important feature that needs to be taken into account. The mixing rule states that the CTE of a two-phase composite is directly proportional to the filler volume percent.²⁶ The composites CTE are calculated as follows in the mixing rule:

$$\alpha_c = f \alpha_f + (1 - f) \alpha_m \quad \dots (3)$$

Table 1 — Water absorbance data for the LLDPE- nano Li_4SiO_4 composite substrate

Sample	Water Absorption (in %)
LLDPE	0.21
LLDPE+ Li_4SiO_4 (2%WF)	0.23
LLDPE+ Li_4SiO_4 (4%WF)	0.24
LLDPE+ Li_4SiO_4 (6%WF)	0.26

Table 2 — Density of LLDPE- nano Li_4SiO_4 composite substrate

Material	CTE (k^{-1})
LLDPE	18×10^{-5}
Li_4SiO_4	1.428×10^{-5}
LLDPE+ Li_4SiO_4 (2%)	17.6696×10^{-5}
LLDPE+ Li_4SiO_4 (4%)	17.3371×10^{-5}
LLDPE+ Li_4SiO_4 (6%)	17.0056×10^{-5}

Where α_f , α_m and α_c are the filler, matrix and composite, CTEs, respectively, and f is the filler volume percent. Table. 3 shows the computed CTE values. From the table it is seen that the change in CTE due to addition of inclusion is minimal up to the %WF of this work.

2.3 Dielectric Characterization

To determine complex permittivity and permeability at X-band frequency, the Nicholson-Ross method is employed.²⁷ The measurement setup includes an Agilent WR-90 X11644A rectangular waveguide line, an Agilent E8362C vector network analyzer, a sample container with a thickness of $\lambda/4$, and an interfacing computer. To decrease errors, the system is calibrated prior to measurements using the thru-reflect-line (TRL) technique.²⁸ Following TRL calibration, LLDPE-nano Li_4SiO_4 composites of dimension $10 \times 22 \times 2 \text{ mm}^3$ are inserted into the sample holder to measure complex permittivity and permeability.

Figure 6 (a&b) illustrates the ϵ' and $\tan\delta_e$ of LLDPE-nano Li_4SiO_4 for 2, 4 and 6 %WFs at X-band frequencies at room temperature. The values for pure LLDPE and Li_4SiO_4 are 2.2 and 6.11, respectively.²⁹ The standard error of ϵ' and $\tan\delta_e$ from its mean is depicted as the error bars in the plots of Fig. 6(a&b). The deviations observed can be due to various reasons such as, casting pressure and formation of

agglomerates of the inclusions in the polymer matrix over the X-band frequency range, the ϵ' is almost constant. The average real permittivity values of the composite with 2%, 4%, and 6% inclusion content are 2.33, 2.48, and 2.55, respectively. The permittivity of the composite substrate shows an incremental trend, as the inclusion content increases. This may be due to inherent electric dipole polarization of Li^+ ions and interfacial polarization due to LLDPE. The presence of Li^+ ions causes polarization in Li_4SiO_4 , as they are strongly polarizable. This increases the Li^+ ions concentration, eventually contribute to the increases in overall permittivity.³⁰ In the complex permittivity investigations, a non-linear behaviour is also observed, which is related to space charge accumulation at the various interfaces created as a result of the heterogeneous composite system of dispersant Li_4SiO_4 in the LLDPE matrix.³¹

The $\tan\delta_e$ of the composite LLDPE-nano Li_4SiO_4 is shown in Fig. 5(b). Dielectric loss is primarily seen due to two types of energy dissipation: conduction loss and dielectric loss. The $\tan\delta_e$ values for the composite LLDPE-nano Li_4SiO_4 vary between 10^{-2} and 10^{-4} with frequency. Negative values of $\tan\delta_e$ in the X-band are seen due to the coupling impact of the host matrix and inclusion in the Fabry-Perot resonance (FPR) region.³² Negative loss tangent values are not always an inherent feature of the material, but they are also affected by the thickness of the substrate.³³ If the substrate thickness is $\lambda/2$, the corresponding FPR may easily alter the connected electromagnetic field and in this work, the sample holder thickness is $\lambda/4$. The unusual behaviour of materials negative loss tangent is explained by Axelrod *et al.*³⁴ The negative loss phenomenon is

Table 3 — Calculated Coefficient of thermal expansion of LLDPE- nano Li_4SiO_4 composite substrate.

Sample	Density(g/cm ³)
LLDPE	0.92
LLDPE+ Li_4SiO_4 (2%)	0.95
LLDPE+ Li_4SiO_4 (4%)	0.98
LLDPE+ Li_4SiO_4 (6%)	1.01

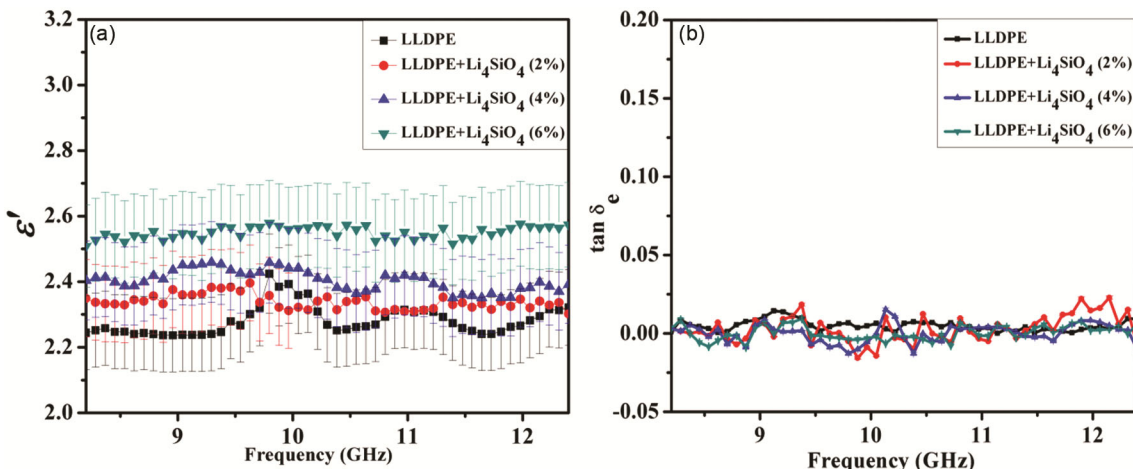


Fig. 6 — (a) Real part of complex permittivity and (b) Dielectric loss tangent of LLDPE- nano Li_4SiO_4 composites.

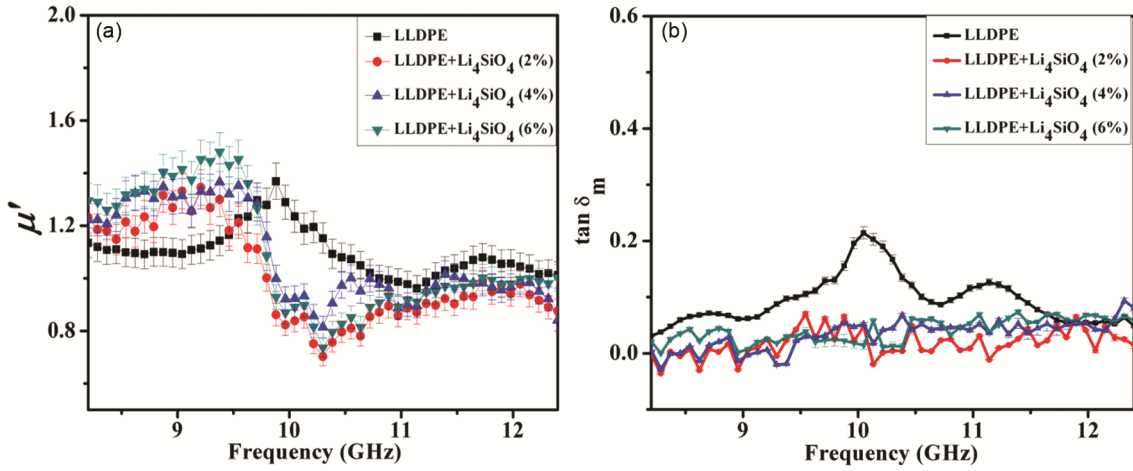


Fig. 7 — (a) Real part of complex permeability and (b) Magnetic loss tangent of LLDPE- nano Li_4SiO_4 composites.

caused by non-compensated matrix-anchored charges inside the polymer matrix and on the interface. Non-bonding orbital's, whether full or empty for positive or negative ions, can cause charge this anchoring. As a result, the molecules reach a metastable state, in which charge separation occurs with energy accumulation. At the suitable frequency, this metastable state can be dissolved, yielding a charge avalanche recombination, resulting in energy release. When this emitted energy exceeds the absorbed, at a specific frequency negative loss phenomenon can be seen.

Figure 7 (a&b) illustrate the real part of complex permeability (μ') and loss tangent ($\tan \delta_m$) for 2%, 4%, and 6% weight fractions of LLDPE- nano Li_4SiO_4 composite. Increasing the inclusion content in the host matrix lowers the average value of from 1.06 to 1.02. This is due to the presence of nonmagnetic Li_4SiO_4 in the nonmagnetic polymer host matrix, which reduces intergranular magnetic interaction. The value of $\tan \delta_m$ fluctuates between 10^{-1} and 10^{-4} .³⁴

3 Return Loss

As the complex dielectric properties are dependent on frequency, role of substrate becomes significant in any high frequency device.³⁵ The relevance of a material for a specific application such as resonator, absorber etc depends on the value of return loss of the material. A low return loss indicates that the material is suitable for absorber applications and on the contrary a high value suggests its suitability for resonator applications (viz. MPAs, dielectric resonator antennas etc). Return losses of pure LLDPE and composites are calculated by using equation (4)

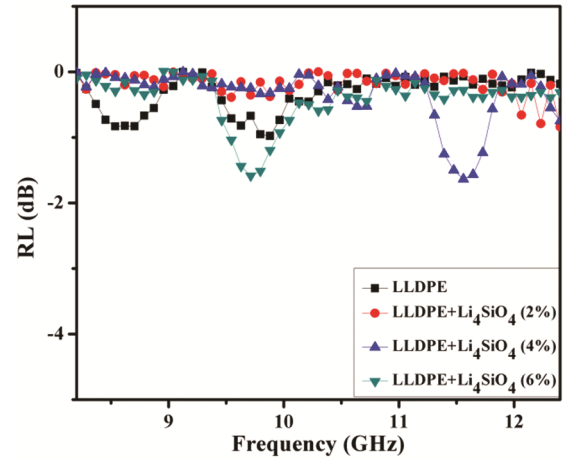


Fig. 8 — Simulated Return Loss of LLDPE- nano Li_4SiO_4 composites.

$$\text{RL}(\text{dB}) = 20 \log_{10} \left| \frac{Z_{\text{in}} - 1}{Z_{\text{in}} + 1} \right| \quad \dots (4)$$

Where,

$$Z_{\text{in}} = \sqrt{\frac{\epsilon_r}{\mu_r}} \tanh \left[j \left(\frac{2\pi f d}{c} \right) \sqrt{\epsilon_r \mu_r} \right] \quad \dots (5)$$

Where Z_{in} is the input impedance in terms of free space, f is the frequency of operation, $d=2$ mm is the substrate thickness and $c = 3 \times 10^8$ m/s is the speed of light.³⁶ The calculated return loss of the composite substrate over the X-band is shown in Fig. 8.

From the figure it is seen that the overall value of return loss for all the composites are lower than -2 dB, suggesting its applicability as substrate for resonators rather than absorber. The estimated RL values complement the complex permittivity values as well. According to the literature, nanocomposites with an RL value of -45dB are suitable for absorber applications.³⁷

4 Conclusions

Li_4SiO_4 nano particles are synthesized following a standard solid state technique. The formation of Lithium orthosilicate is confirmed by diffraction peaks obtained in the XRD spectra. The Li–O–Li stretching vibrations and Si–O–Si bending vibrations observed from FTIR measurements also confirms the same. The TEM images reveal the nanoparticles average size as ~ 150 nm. The SEM images show that the inclusions in LLDPE are evenly distributed. The complex permittivity exhibits a linear trend with low fluctuations which can be attributed to buildup of space charge at the inclusion-polymer interfaces. The ϵ' and $\tan\delta_e$ are in the range of 2.2 – 2.6 and 10^{-2} – 10^{-4} respectively. The study reveals that, the composite can be used as a substrate material for various devices such as microstrip patch antenna, dielectric resonators etc. The moderate values of ϵ' , and the computed RL values complements the same.

Acknowledgement

Authors would like to acknowledge, Prof. Nidhi S Bhattacharya, Department of Physics, Tezpur University (Central), Assam, for the support and guidance provided for carrying out some of the experimental works reported in this work. The authors declare that no funds, grants, or other support were received for carrying out this research work.

References

- Sebastian M T, Ubic R & Jantunen H, *Int Mater Rev*, 60 (2015) 392.
- Fu S, Sun Z, Huang P, Li Y & Hu N, *Nano Mater Sci*, 1 (2019) 2.
- Zhang C, Zuo R, Zhang J & Wang Y, *J Am Ceram Soc*, 98 (2015) 3.
- Anjana P S, Sebastian M T, Suma M N & Mohanan P, *Int J Appl Ceram Technol*, 5 (2008) 325.
- Peng H, Ren H, Dang M, Zhang Y, Gu Z, Yao X & Lin H, *J Mater Sci: Mater Electron*, 30 (2019) 6680.
- Sarmah D, Bhattacharyya N S & Bhattacharyya S, *IEEE Trans Dielectr Electr Insul*, 20 (2013) 1845.
- Pant H C, Patra M K, Verma A, Vadera S R & Kumar N, *Acta Mater*, 54 (2006) 3163.
- Rajesh S, Nisa V S, Murali K P & Ratheesh R, *J Alloys Compd*, 477 (2009) 677.
- Murali K P, Rajesh S, Prakash Om, Kulkarni A R & Ratheesh R, *Mater Chem Phys*, 113 (2009) 290.
- Hu T, Juuti J, Jantunen H & Vilkmann T, *J Eur Ceram Soc*, 27 (2007) 3997.
- Drishya V, Unnimaya A N, Naveenraj R, Suresh E K & Ratheesh R, *Int J Appl Ceram Technol*, 13 (2016) 810.
- Jeon C J & Kim E S, *J Korean Ceram Soc*, 48 (2011) 257.
- George S S, Raman S, Mohanan P & Sebastian M T, *In 2010 Indian Antenna Week: A Workshop on Adv. Antenna Tech*, 1 (2010).
- Zhang L, Zhang J, Yue Z & Li L, *AIP Adv*, 6 (2016) 95319.
- Palukuru V K, Sonoda K, Surendran R & Jantunen H, *Prog Elect Res C*, 16 (2010) 195.
- Seki T, Yamamoto H, Hori T & Nakatsugawa M, *IEEE MTT-S Int Microwave Symp Digest*, 1 (2001) 385.
- Gogoi P J, Bhattacharyya S & Bhattacharyya N S, *J Electron Mater*, 44 (2015) 1071.
- Chun K S, Husseinsyah S & Syazwani N F, *J Thermoplast Compos Mater*, 29 (2016) 1641.
- He J, Ye H, Liu S & Zhao J, *Polym Polym Compos*, 14 (2006) 611.
- Kamutzi F, Schneider S, Barowski J, Gurlo A, Dorian A & Hanaor H, *J Eur Ceram Soc*, 41 (2021) 3879.
- Wu X, Wen Z, Xu X, Wang X & Lin J, *J Nucl Mater*, 392 (2009) 471.
- Dutta P, Saikia B, Alapati P R & Borah K, *J Electron Mater*, 50 (2021) 1434.
- Patterson A L, *Phys Rev*, 56 (1939) 978.
- Hafidz N S B M, Rehan M S B M & Mokhtar H B, *Mater Today*, 48 (2022) 720.
- Bensch J J & Brynard H J, *Nature Phys Sci*, 239 (1972) 96.
- Thomas S, Deepu V, Uma S, Mohanan P, Philip J & Sebastian M T, *Mater Sci Eng: B*, 163 (2009) 67.
- Nicolson A M & Ross G F, *IEEE Tran Instrum Meas*, 19 (1970) 377.
- Engen G F & Hoer C A, *IEEE Trans Microw Theory Technol*, 27 (1979) 987.
- Liang F, Sun C, Yang H, Li E & Zhang S, *J Mater Sci: Mater Electron*, 28 (2017) 15405.
- Ozah S & Bhattacharyya N S, *J Magn Magn Mater*, 342 (2013) 92.
- Ahmad A F, Abbas Z, Obaiys S J & Abdalhadi D M, *Polymers*, 9 (2017) 12.
- Karpisz T, Salski B, Kopyt P & Krupka J, *IEEE Trans Microw Theory Technol*, 67 (2019) 1901.
- Zhang K L, Hou Z L, Kong L B, Fang H M & Zhan K T, *Chin Phys Lett*, 34 (2017) 097701.
- E Axelrod E, Puzenko, Haruvy Y, Reisfeld R & Feldman Y, *J Non-Cryst Solids*, 352 (2006) 4166.
- Geyer R G, *Dielectric characterization & reference materials*, US Department of Commerce NIST, (1990) 3.
- Kumar R, Choudhary H K, Pawar S P, Bose S & Sahoo B, *Phys Chem Chem Phys*, 19 (2017) 23268.
- Choudhary H K & Sahoo B, *J Conv Technol*, 3 (2017) 918.